On the Existence and Uniqueness of Minimum Time Optimal Trajectory for a Micro Air Vehicle under Wind Conditions

Ram V. Iyer, Rachelle Arizpe, Phillip R. Chandler

Abstract An important subproblem in the area of cooperative control of multiple, autonomous, unmanned air vehicles is the determination of the minimum-time optimal paths for the agents to fly from one destination to the next. The tasks for the air vehicles are usually tightly coupled in time, and hence estimates of the times taken for each air vehicle to fly from one destination to the next is highly critical for correct assignment of tasks. In this article, we discuss the existence and uniqueness of minimum time solutions for the trajectory planning problem for a Micro Air Vehicle (MAV) under wind conditions. We show that there exists a minimum time solution for the trajectory planning problem with a minimum turn radius constraint for the air vehicle, and for a non-zero, time-varying wind vector field satisfying certain easily checked sufficient conditions. We also prove uniqueness for almost every combination of initial and final conditions in the case of a wind vector field that can vary with time but is constant in the spatial variable at each time instant.

1 Introduction

Cooperative Control of multiple, autonomous unmanned air vehicles (UAVs) is an active area of research that holds enormous potential for military and civilian applications [1, 2, 3]. This new paradigm for control has been implemented in the MultiUAV simulation platform by the Air Force Research Laboratory [3]. The Mul-

R. V. Iyer
Department of Mathematics and Statistics, Texas Tech University, Lubbock, TX 79409-1042, e-mail: ram.iyer@ttu.edu
R. Arizpe
Antonian College Preparatory, 6425 West Ave San Antonio, Texas 78213, e-mail: rarizpe@antonian.org.
P. Chandler
U.S. Air Force Research Laboratory, Wright-Patterson Air Force Base, Ohio 45433-7531, e-mail: phillip.chandler@wpafb.af.mil

tiUAV platform has a hierarchical architecture, in which, at the highest level the dynamics of the controlled agents are suppressed, and a task allocation for the agents is performed using graph theory. The tasks for the agents are usually tightly coupled in time [3, 4], and hence estimates of the times taken for each agent to fly from one destination to the next is highly critical for correct assignment of tasks. This estimate of times is usually obtained by considering a kinematic model of the air vehicle, along with kinematic turn-radius constraints, to keep the computation time at a manageable level [5, 6, 7]. The key result that is used in this computation is Dubins' result on the existence of minimum time solutions for a kinematic model with minimum turn-radius constraint [8]. However, this result is only for valid for zero-wind, and hence all of the available cost estimation algorithms are only valid for zero-wind.

In this article, we discuss the existence and uniqueness of minimum time solutions for the trajectory planning problem for a Micro Air Vehicle (MAV) under wind conditions. Numerical results from algorithms based on this paper can be found in [10]. MAV's are powered by batteries that typically have a very short life [2, 5]. Therefore, before deployment, it is desirable to know: (a) whether the MAV can complete its mission - which requires flight from Point A with velocity V_0 to Point B with velocity V_f, , in the presence of wind; (b) if the answer to the previous item is in the affirmative, then the control inputs that achieve the mission. We model an MAV flying with a constant speed in the wind axes and at a constant altitude. The kinematic equations of motion for the MAV are:

$$\dot{x} = V(\cos\theta, \sin\theta) + W(x,t); \quad \dot{\theta} = u. \tag{1}$$

where $x = (x_1, x_2)$, $W(x,t) = (W_1(x,t), W_2(x,t))$, and $W_i(x,t)$; $i = 1,2$ are functions with bounded derivatives. These equations contain the wind vector field that is not considered in earlier works [5, 8, 6, 7, 9]. Let $q = (x, \theta)$. The initial and final time constraints are: $q(0) = q_0$ and $q(t_f) = q_f$ where t_0 is fixed and t_f is free. The constraint on the piecewise continuous input function $u(\cdot)$ arising from a constraint on the minimum turn-radius for the MAV is:

$$|u(t)| \leq u_{max} = \frac{V}{R_{min}}, \tag{2}$$

for all t. Here R_{min} is the minimum turn radius *in the absence of wind* and arises due to mechanical limitations on the aircraft. Even for such a simple model the question of existence of time-optimal trajectories is unknown in the presence of wind. In the absence of wind (that is $W(x,t) = (0,0)$), the well-known Dubins' theorem [8] posits the existence of a time-optimal solution for any initial and final positions and velocities of the aircraft on a plane, when the aircraft is flying with constant speed and has a minimum turn radius constraint. For a non-zero, time-varying wind vector field satisfying certain technical conditions, we provide easily checked sufficient conditions under which a time-optimal solution exists. The verification of these conditions can then be used as the starting point for a numerical algorithm to compute the time-optimal trajectory. In the case of wind that is only a function of time (and

independent of the space variable) we show that the solution is unique except for initial and final states taking values on a set of measure zero. For more general wind vector fields, the question of uniqueness is still to be investigated. To prove the existence of a time optimal solution, we do not use perturbation techniques around the zero wind condition for which the solution is known to exist. Instead, we use Filippov's theorem on the existence of a solution in conjunction with Dubin's result for zero wind.

We are given the initial and final positions and orientations for the MAV, and the problem is to find the minimum time path connecting the initial and final states. As the speed of the aircraft increases due to a tail wind, one would expect the instantaneous minimum turn radius to increase as well. It is easy to check that if $\|\dot{x}\| > V$ for some (x,t) then $\|\dot{x}\| = R'_{min}(x,t)$ max $|\dot{\theta}| = R'_{min}(x,t)\,u_{max}$, along with $V = R_{min}\,u_{max}$ implies $R'_{min}(x,t) > R_{min}$, as required.

As is well known, the minimum time trajectory planning problem can be cast as an optimal control problem for the sake of numerical solution [13]. Direct and indirect methods are usually employed to solve the optimal control problem [13]. Such methods assume the existence of the optimal solution and use gradient-based techniques to find the solution. For the minimum-time problem for the no wind case, we can show using Dubins' theorem [8] that the length of the trajectory (which is proportional to the minimum time) is a discontinuous function of the final state when the initial state is held fixed. To be specific, if the initial position and velocity is fixed, then the length of the minimum time path is a discontinuous function of the final position and velocity. Recall, that the magnitude of the velocity is fixed and only the direction is a variable. We show that the discontinuities are of the first-kind - that is, they are simple jump discontinuities. This implies that numerical methods must be carefully initialized for convergence. In the next section, we study the aspects of the solution for the no wind case paying careful attention to two issues: nonuniqueness of solutions and discontinuity of the solution. For the special case of constant wind vector field, we show using coordinate transformations that the qualitative nature of the solutions is the same as the zero wind case, and hence we can expect both discontinuous and non-unique solutions.

2 Discussion of Dubins' Theorem for the zero wind case

Dubins' theorem [8] establishes the existence of a solution to the minimum time optimal control problem for the special case $W(x,t) = (0,0)$ for all $x \in \mathbb{R}^2$ and $t \in \mathbb{R}_+$. This theorem states that for every initial, final positions and velocities the minimum time solution is an arc-line-arc or arc-arc-arc solution. As the minimum time solution is invariant with respect to translations and rotations of the coordinate axis, we can change coordinates so that the initial position is at the origin of $\mathbb{R}^2$ and the final position is at $(l,0)$ on the ordinate axis. The initial and final velocity directions measured with respect to this axis are termed ϕ_0 and ϕ_f respectively in Figures 1 - 3. To understand the behavior of the minimum time solution as a function

of the initial and final states, we considered - without loss of generality - the initial state to be fixed, and varied the final states. As the final state comprises of the final position and the final direction for the velocity vector, we consider each change in turn.

The direction of the velocity induces an orientation on the circles tangent to the velocity vector. In all the figures, we denote the center of the counterclockwise oriented circle by Z_0 and Z_f respectively, while the centers of the clockwise oriented curves are denoted by Y_0 and Y_f respectively. Thus we can distinguish between the Z_0LY_f from the Y_0LZ_f arc-line-arc solutions etc. This distinction is important in what follows. It turns out that for each ϕ_0 and ϕ_f one can compute a critical separation l_c such that only arc-line-arc solutions can exist for $l > l_c$ (see Appendix I). Below, we will fix the initial and final positions at points T and S respectively; fix the initial velocity direction ϕ_0; and vary the final velocity direction ϕ_f (see Figures 1 - 3). There are primarily three cases to consider:

1. $l = \|x_f - x_0\| > l_c$.
2. $0 < l \leq l_c$;
3. $l = 0$.

Case 1: Please refer to Figure 1. In this case, $l > l_c$; the circles Y_0, Z_0 and Y_f, Z_f do not intersect even at a single point; and hence the trajectories are always of the arc-line-arc type. We further observe that:

- the length of the minimum time solution is a continuously differentiable function of the angle ϕ_f;
- the solution changes from Y_0LZ_f to Z_0LY_f as the angle goes through specific angle ϕ_f^*. The exact value of ϕ_f^* is not as important as its property – it is the angle for which two minimum time solutions exist (see Fig. 1(c)). As the solution changes from Y_0LZ_f to Z_0LY_f for $\phi_f > \phi_f^*$, its length changes in a continuous manner as a function of ϕ_f.
- As ϕ_f increases beyond ϕ_f^* the solution is of the type Z_0LY_f (see Fig. 1(d)) until $\phi_f = \phi_c$ when we have a LY_f solution (see Fig. 1(e)).
- For $\phi_c < \phi_f < 2\pi$, the solution is of the type Y_0LY_f.

To re-emphasize, when $l > l_c$, the minimum length remains continuous function of ϕ_f.

Case 2: Please refer to Figure 2. In this case, $0 < l \leq l_c$. Hence, intersections of the circles Y_0 or Z_0 with either Y_f or Z_f is possible. This leads to two phenomena not observed in the previous case:

- A discontinuous change in the length of the minimum time trajectory at two critical angles (one of which is shown in Figure 2(b) and the other in Figure 2(h)). At the angle $\phi_f = \bar{\phi}_c$ in Figure 2(b)), the circle Z_f touches Y_0 and hence the Y_0LZ_f solution has a line section of zero length. As ϕ_f increases from $\bar{\phi}_c$, the solution switches to a Z_0LY_f solution shown in Figure 2(c).
- Appearance of arc-arc-arc solutions for ϕ_f satisfying: $\phi_f \in [\tilde{\phi}_c, \hat{\phi}_c]$. The lengths of the solutions, vary continuously as the arc-arc-arc solutions appear or disappear.

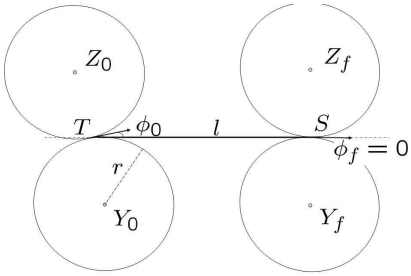

(a) A Y_0L solution for $\phi_f = 0$.

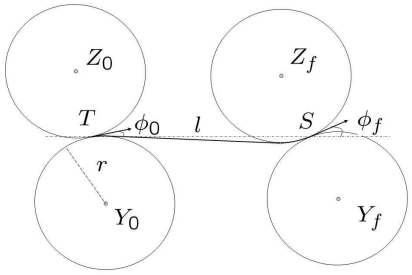

(b) A Y_0LZ_f solution for $0 < \phi_f < \phi_f^*$.

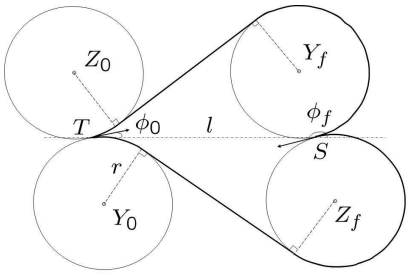

(c) Two minimum time Y_0LZ_f and Z_0LY_f solutions when $\phi_f = \phi_f^*$.

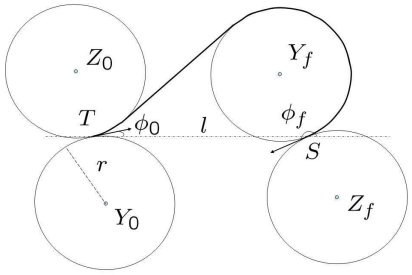

(d) A Z_0LY_f solution for $\phi_f^* < \phi_f < \phi_c$.

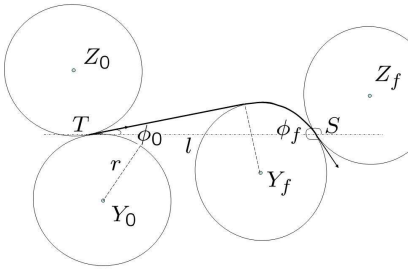

(e) A minimum time LY_f solution when $\phi_f = \phi_c$.

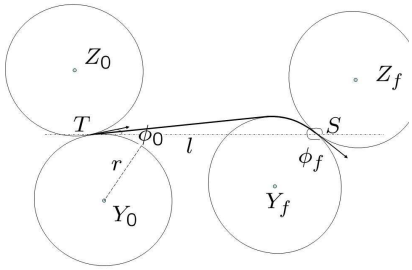

(f) A minimum time Y_0LY_f solution when $\phi_c < \phi_f < 2\pi$.

Fig. 1 Variation of the minimum time solution with the final angle ϕ_f for $l \geq r(3 + |\sin\phi_0|)$.

- Just as in Case 1, for $\phi_f = \phi_f^*$ we see the appearance of two arc-arc-arc solutions of equal length as shown in Figure 2(f). The lengths of the solution changes in a continuous manner as a function of ϕ_f.
- As mentioned in the first item of this case, when $\phi_f = \bar{\phi}_c'$ in Figure 2(h)), the circle Y_f touches Z_0 and hence the Z_0LY_f solution has a line section of zero length. When the angle ϕ_f is decreased from this value, then the length of the minimum time solution changes discontinuously.

This discussion shows that the minimum time solution for Case 2 is unique and its length is a continuously differentiable function of ϕ_f for fixed l and ϕ_0 is fixed, except for at most four values.

Case 3: Please refer to Figure 3. In this case, $l = 0$. As the initial and final positions coincide, there is no angle ϕ_f for which an arc-line-arc solution with a non-zero line segment is possible. The solutions for all angles ϕ_f can be considered to be arc-arc-arc solutions. The solutions are unique except for the case $\phi_f = \phi_0 + \pi$.

Instead of varying the final angle ϕ_f while holding l fixed, we can vary l with ϕ_f fixed. We can for example reduce l from a large value greater than the critical separation l_c. Then the same arguments presented above still apply. The crux of the matter is that the minimum time solution for the zero wind case is *unique* and is a continuously differentiable function of ϕ_f and l when ϕ_0 is fixed, except for at most four points. These features persist for the important case of non-zero, time-varying wind vector field that is constant in the spatial coordinate, as will be seen later.

3 Existence of minimum time solution

Next, we will show that there exists a solution to the minimum time optimal control problem even when the wind is non-constant, time-varying and satisfying two constraints. First, it is clear that there must be a bound on the wind speed so that the aircraft is able to fly upwind. This assumption is needed for *reachability*, that is, for a solution to exist. We will also need a bound on the rate of change of the wind due to the bound on u Specifically, we will assume that W is a Lipschitz continuous function of t and x (which implies it is differentiable almost everywhere by Rademacher's Theorem [11]). Furthermore, suppose that:

A-1. $\|W\|_\infty = \sup_{x,t} \|W(x,t)\| < V$.

A-2. $\|\frac{\partial W}{\partial t}\|_\infty + \|\frac{\partial W}{\partial x}\|_\infty (V + \|W\|_\infty) \leq \beta \sqrt{V^2 - \|W\|_\infty^2}\, u_{max}$,

where: $\|\frac{\partial W}{\partial t}\|_\infty = \sup_{x,t} \|\frac{\partial W}{\partial t}(x,t)\|_2$ and $\|\frac{\partial W}{\partial x}\|_\infty = \sup_{x,t} \|\frac{\partial W}{\partial x}(x,t)\|_2$, and $0 < \beta < 1$ is some constant.

Theorem 1. *Suppose that $W(x,t)$ is a time-varying (Carathéodory) vector field of wind velocities satisfying assumptions A1 - A2. Then there exists a solution to the minimum time optimal control problem for the system (1).*

Proof: The theorem is proved using Filippov's Theorem [14] on minimum time optimal control. A special case of this theorem applicable to our problem is given in the Appendix as Theorem 2. This theorem requires that the set $Q = [-u_{max}, u_{max}]$ be convex which is true. Due to our assumptions on $W(x,t)$, the function $f(q,t,u) = [V\cos\theta + W_1(x,t)\ V\sin\theta + W_2(x,t)\ u]^T$ is differentiable a.e. with an essentially bounded derivative in $q = (x,\theta)$ and continuous in t. The requirement that $q^T f(q,t,u) \leq C(\|q\|^2 + 1)$ for some $C > 0$ is true by the following:

$$\begin{aligned} q^T f(q,t,u) &= V\langle x,(\cos\theta,\sin\theta)\rangle + \langle x,W(x,t)\rangle + \theta u \\ &\le V\|x\|_2 + \|W(x,t)\|_2\|x\|_2 + |\theta| u_{max} \\ &\le 2V\|x\|_2 + |\theta| u_{max} \\ &\le \max\{2V,u_{max}\}(\|x\|_2 + |\theta|) \\ &\le \sqrt{2}\max\{2V,u_{max}\}\sqrt{\|x\|_2^2 + |\theta|^2} \\ &\le \sqrt{2}\max\{2V,u_{max}\}(\|q\|^2+1). \end{aligned}$$

As required by Filippov's theorem, we will demonstrate that one solution exists to the trajectory planning problem by modifying a Dubins' solution for the zero-wind case.

Setting the wind vector field to be identically zero, let $r(\tau) = (z(\tau),\theta(\tau))$ be the Dubins' solution (modulo identification) with minimum turn-radius $R \ge R_{min}$ where

$$R = \frac{R_{min}\left(\|W\|_\infty + V\right)^2}{(1-\beta)V^2}. \tag{3}$$

We will show later that this value of R allows the modified trajectory to satisfy the constraint $|u(t)| \le u_{max}$. The variable τ used to denote the Dubins' solution is proportional to the arc-length along this solution with proportionality constant V. Hence, the function $r(\cdot)$ satisfies $r(0) = q_0$ and $r(\tau_f) = q_f$ for some τ_f. The initial condition $\theta_{\text{no wind}}(0)$ for the zero-wind case has to be chosen different from $\theta(0)$ because at the initial time the aircraft is only capable of flying in the direction of $Z = W(x(0),0) + V(\cos\theta(0),\sin\theta(0))$ and not $V(\cos\theta(0),\sin\theta(0))$. The angle $\theta_{\text{no wind}}(0)$ is chosen according to: $Z = \|Z\|(\cos\theta_{\text{no wind}}(0),\sin\theta_{\text{no wind}}(0))$. Using this solution, we will obtain a solution to the trajectory planning problem when $W(x,t) \ne (0,0)$.

Let T be the unit vector tangent and N be the unit normal vector to the Dubins' solution at a generic point $r(\cdot)$. In other words, $T = \frac{1}{\|\frac{dz}{d\tau}\|}\frac{dz}{d\tau}$. Select N so that it is the *outward pointing* normal at the point $z(\tau)$ (see Figure 4). By Dubins' theorem [8], T is a piecewise continuous function.

We will construct a solution that will traverse the same points $r(\cdot)$ at times t, that is, $q(t) = r(\tau)$ for some t and τ. Consider the following differential equation for the time variable t:

$$\frac{dt}{d\tau} = \frac{V}{\sqrt{V^2 - \|W(z(\tau),t(\tau)\|^2 + W_\parallel^2(\tau)} + W_\parallel(\tau)}; \quad t(0) = 0, \tag{4}$$

where

$$W_\parallel(\tau) \stackrel{\triangle}{=} W(z(\tau),t(\tau))\cdot T(z(\tau)).$$

The differential equation (4) has a unique solution on $[0,\tau_f]$ because the denominator on the right hand side is strictly greater than zero by Assumption A-1 and hence is Lipschitz continuous almost everywhere as a function of τ. As the right hand side

of (4) is strictly greater than zero, t is a monotone increasing, Lipschitz function of τ. Denote $t_f \stackrel{\triangle}{=} t(\tau_f)$. By the previous discussion, for every $\hat{t} \in [0, t_f]$, there exists a $\tau \in [0, \tau_f]$ such that $\hat{t} = t(\tau)$. By a slight abuse of notation, we will denote both $\hat{t}$ and t by t in the following.
For any $t \in [0, t_f]$, denote:

$$\begin{aligned}
\bar{V}(t) &\stackrel{\triangle}{=} V(\cos\theta(t(\tau)), \sin\theta(t(\tau))), \\
\bar{V}_{\|}(t) &\stackrel{\triangle}{=} \bar{V}(t) \cdot T(z(\tau)), \\
\bar{V}_{\perp}(t) &\stackrel{\triangle}{=} \bar{V}(t) \cdot N(z(\tau)) \\
W_{\perp}(t) &\stackrel{\triangle}{=} W(z(\tau), t(\tau)) \cdot N(z(\tau)).
\end{aligned}$$

To obtain the control law for one solution to the trajectory planning problem, set $\theta(t)$ to be such that:

$$\bar{V}_{\perp}(t) = -W_{\perp}(t). \tag{5}$$

As there is a constraint on $\dot{\theta}$ (see (2)), it has to be shown that such a choice of $\theta(t)$ can be made without violating the constraint. This is where the assumption A-2 is needed.

Define $\xi(t) \stackrel{\triangle}{=} \bar{V}_{\perp}(t) + W_{\perp}(t)$. At $t = 0$, we can select $\theta(0)$ so that $\xi(0) = 0$ due to the assumption A-1. Thereafter, we need to show that one can choose $u(t)$ so that $\frac{d\xi}{dt} = 0$. This will imply $\xi(t) = 0$ or (5) is true. Now, we have the following basic identities for $T(t)$ and $N(t)$:

$$\begin{aligned}
T(t) \cdot T(t) = 1 &\Longrightarrow T(t) \cdot \frac{dT}{dt} = 0 \\
N(t) \cdot N(t) = 1 &\Longrightarrow N(t) \cdot \frac{dN}{dt} = 0 \\
T(t) \cdot N(t) = 0 &\Longrightarrow T(t) \cdot \frac{dN}{dt} + \frac{dT}{dt} \cdot N(t) = 0
\end{aligned}$$

From the above equations and noting the planar nature of the curves, we get:

$$\frac{dT}{dt} = -\omega N \tag{6}$$

$$\frac{dN}{dt} = \omega T \tag{7}$$

where ω is either 0, $\frac{\bar{V}_{\|}+W_{\|}}{R}$ or $-\frac{\bar{V}_{\|}+W_{\|}}{R}$ because $\bar{V}_{\|} + W_{\|}$ is the tangential component of the velocity (that is $\dot{x} \cdot T$) along the Dubins solution. At the end of the proof, it will become clear why ω must take these values. For example, in the case depicted in Figure 4, we have $\omega = \frac{\bar{V}_{\|}+W_{\|}}{R}$ because $\frac{dT}{dt}$ is directed in the opposite direction to N.

Therefore:

$$\begin{aligned}\frac{d\xi}{dt} &= \frac{dW}{dt}\cdot N + W\cdot\frac{dN}{dt} + \frac{d\bar{V}}{dt}\cdot N + \bar{V}\cdot\frac{dN}{dt}\\ &= \omega(W+\bar{V})\cdot T + \frac{dW}{dt}\cdot N + \frac{d\bar{V}}{dt}\cdot N\\ &= \omega(W_{\|}+\bar{V}_{\|}) + \frac{dW}{dt}\cdot N + \frac{d\bar{V}}{dt}\cdot N \end{aligned} \tag{8}$$

We now observe that:

$$\frac{d\bar{V}}{dt} = V\left(-\sin\theta,\cos\theta\right)\dot{\theta} = V\left(-\sin\theta,\cos\theta\right)u$$

Let $\mu(t) = \text{sign}\left(\left(-\sin\theta,\cos\theta\right)\cdot N\right)$. Observe that $\mu(\cdot)$ is a piecewise function of t because N is a piecewise continuous function of t. We pick $u(t)$ to be:

$$u(t) = -\mu\frac{1}{\bar{V}_{\|}}\left(\omega\left(W_{\|}+\bar{V}_{\|}\right) + \frac{dW}{dt}\cdot N\right). \tag{9}$$

We show that the choice of $u(t)$ leads to $\frac{d\xi}{dt} = 0$. First, observe that (see Figure 4):

$$\left|V\left(-\sin\theta,\cos\theta\right)\cdot N\right| = \bar{V}\cdot T = \bar{V}_{\|} \tag{10}$$

Substituting (9) and (10) into (8) we get:

$$\begin{aligned}\frac{d\xi}{dt} &= \omega(W_{\|}+\bar{V}_{\|}) + \frac{dW}{dt}\cdot N + V\,u\left(-\sin\theta,\cos\theta\right)\cdot N\\ &= \omega(W_{\|}+\bar{V}_{\|}) + \frac{dW}{dt}\cdot N - \left(\omega\left(W_{\|}+\bar{V}_{\|}\right) + \frac{dW}{dt}\cdot N\right)\\ &= 0\end{aligned}$$

All of the quantities on the right hand side of (9) are known at time t. More importantly, $u(\cdot)$ is a measurable function of t because each of the functions on the right hand side is measurable, and the denominator is always greater than zero by Assumption A-1 and $\xi(t) = 0$.

Next, we show that $|u(t)| \leq u_{max}$ for R chosen as in (3). For this, first observe that the minimum value of $V_{\|}$ is achieved when $W(x,t)$ is directed orthgonal to T and furthermore $|W(x,t)| = \|W\|_{\infty}$. In this case, $\bar{V}_{\|} = \sqrt{V^2 - \|W\|_{\infty}^2}$.

$$\begin{aligned}
|u(t)| &= \frac{1}{|\bar{V}_{\|}|}\left|\omega(W_{\|}+\bar{V}_{\|})+\frac{dW}{dt}\cdot N\right| \\
&\leq \frac{(W_{\|}+\bar{V}_{\|})^2}{R\,|\bar{V}_{\|}|}+\frac{\|\frac{dW}{dt}\|\,\|N\|}{\sqrt{V^2-\|W\|_{\infty}^2}} \\
&= \frac{(W_{\|}+\bar{V}_{\|})^2}{R\,|\bar{V}_{\|}|}+\frac{\|\frac{\partial W}{\partial t}+\frac{\partial W}{\partial x}(\bar{V}+W)\|}{\sqrt{V^2-\|W\|_{\infty}^2}} \\
&\leq \frac{(W_{\|}+\bar{V}_{\|})^2}{R\,|\bar{V}_{\|}|}+\beta\,u_{max},
\end{aligned}$$

where the last inequality is due Assumption A-2. It is proved in the Appendix 4 that:

$$\max_{V_{\perp}=-W_{\perp}} \frac{(W_{\|}+\bar{V}_{\|})^2}{|\bar{V}_{\|}|} = \frac{(\|W\|_{\infty}+V)^2}{V}.$$

This yields:

$$|u(t)| \leq \frac{(\|W\|_{\infty}+V)^2}{RV}+\beta\,u_{max}.$$

As $R = \frac{1}{u_{max}(1-\beta)}\frac{(\|W\|_{\infty}+V)^2}{V} = \frac{R_{min}(\|W\|_{\infty}+V)^2}{(1-\beta)V^2}$, we have $|u(t)| \leq u_{max}$.

Now that existence of one solution with a measurable control has been shown, let us see what form $\dot{x}$ takes for this solution:

$$\begin{aligned}
\dot{x} &= \bar{V}(t)+W(\phi(t),t) \\
&= \bar{V}_{\|}(t)\,T+\bar{V}_{\perp}(t)\,N+W_{\|}(t)\,T+W_{\perp}(t)\,N \\
&= (\bar{V}_{\|}(t)+W_{\|}(t))\,T. \qquad (11)
\end{aligned}$$

Using the time variable τ for the Dubins' solution, we have:

$$\frac{dx}{d\tau} = V\,T(\tau).$$

Comparing the last two equations, we must have

$$\frac{dt}{d\tau} = \frac{V}{\bar{V}_{\|}+W_{\|}}.$$

Using a similar argument that was used to obtain (6 - 7), we get for the Dubins' solution:

$$\frac{dT}{d\tau} = -\kappa N \qquad (12)$$

$$\frac{dN}{d\tau} = \kappa T \qquad (13)$$

where κ is either 0, $\frac{V}{R}$ or $-\frac{V}{R}$, because the Dubins' solution either has lines or curves with constant turn radius R. From Equation (4) and (12), we obtain:

$$\frac{dT}{dt} = \frac{dT}{d\tau}\frac{d\tau}{dt} = -\kappa\frac{\bar{V}_{\|}+W_{\|}}{V}N$$

which is consistent with Equation (6) and the constant ω that was introduced there.

This concludes shows the existence of a solution when the wind speed is not zero.

Now consider the set of pairs all solutions and the final times: $S = \{(q(\cdot),t_f)\,|\,q(0) = q_0; q(t_f) = q_f; t_f \in \mathbb{R}_+\}$. We know that this set is non-empty. The elements of this set can be ordered according to the final times t_f. There must exist a minimal element $(q^*(\cdot),t_f^*)$ by a special case of Filippov's Theorem [14](See Appendix). □

Remarks: Notice that when the wind is constant with speed W, then one can choose $\beta = 0$ in A-2. Then for the Dubins' solution for the existence part, $R = \frac{1}{u_{max}}\frac{(W+V)^2}{\sqrt{V^2-W^2}}$. In particular, when the constant wind has zero speed, we have $R = \frac{1}{u_{max}}V = R_{min}$.

We present a simple numerical example to illustrate the method used to show existence of one solution. Consider a MAV with $V = 50$, minimum turn radius $R_{min} = 35$ and constant wind $W(x,t) = 25\,(1,1)$. Then according to the remarks after Theorem 1, we can choose $R = R = R_{min}\frac{(W+V)^2}{V^2} = 102$. The Dubins solution with no wind and $R = 102$ is shown in Figure 5(a). The path is based on an Arc-Arc-Arc solution from coordinates $(35,76,0.5)$ to $(24,85,\frac{\pi}{4})$. The step-size used was 0.1 and this path took 158 steps to travel. The next two figures are different scenarios of a constant wind. The dark arrow symbolizes the wind direction. In each figure, the spacing is wider where the wind seems to be helping the trajectory of the MAV.

Figure 5(b) represents $W = (25,25)$, which is wind directed toward the first quadrant. With the same step-size, travel on this path took 546 steps.

3.1 Uniqueness of the solution for a special wind vector field

Suppose the wind $W(x,t) = W(t)$ depends only on the time variable, while still satisfying the conditions (A-1) - (A-2). Then, we can the transform coordinates (with the same time variable) as follows:

$$\bar{x} = \varphi(x,t) = x - \int_0^t W(s)\,ds \quad \text{and} \quad \bar{\theta} = \theta. \tag{14}$$

In the new coordinates $(\bar{x},\bar{\theta})$, the equations take on the form:

$$\dot{\bar{x}} = V(\cos\bar{\theta},\sin\bar{\theta}); \quad \dot{\bar{\theta}} = u. \tag{15}$$

which is of the form considered by Dubins. We had seen earlier that except for $\phi_f = \phi_0 + \pi$ (where we have employed the notation in Figures 1, 2, 3), the minimum time solution is unique. Even for the case $\phi_f = \phi_0 + \pi$, it is natural to identify the two solutions, leaving us with unique minimum time solutions for all combinations of initial, final positions and velocity directions. Therefore, in the coordinates $(\bar{x}, \bar{\theta})$, there exists a unique minimum time solution for all initial, final states. The inverse transform is obviously:

$$x = \vartheta(\bar{x}, t) = \bar{x} + \int_0^t W(s)\, ds \quad \text{and} \quad \theta = \bar{\theta}. \tag{16}$$

There exists a minimum time solution by Theorem 1 for the original problem with final states (x_f, θ_f). Let us denote this solution by $q^*(t) = (x^*(t), \theta^*(t))$ with minimum time t_f^*. In the new coordinates, the final states are $(\bar{x}_f, \bar{\theta}_f)) = (x_f - \int_0^{t_f^*} W(s)\, ds, \theta_f)$. There exists a unique Dubins' solution in the new coordinates with final time t_f. If $t_f \neq t_f^*$, then on inverse transformation, the point $(\bar{x}_f, \bar{\theta}_f))$ transforms to $(\bar{x} + \int_0^{t_f} W(s)\, ds, \theta_f) \neq (x_f, \theta_f)$ which is a contradiction. Hence $t_f = t_f^*$, and the minimum time solutions in the initial and transformed coordinates are simply transformations of each other. As the solution in the transformed coordinates is unique, the solution in the original coordinates are also unique.

4 Conclusion

In this paper, we have shown that a minimum time solution for the trajectory planning problem for a micro air vehicle with a minimum turn radius constraint in the presence of a non-zero, time-varying wind vector field exists. For a non-zero, time-varying wind vector field, we provide easily checked sufficient conditions under which a time-optimal solution exists. We also shown uniqueness for almost every initial and final conditions for the case of a wind vector field that varies with time, but is constant in the spatial variable for each time instant. These results are of critical importance in proving convergence of numerical algorithms for trajectory planning [10].

APPENDIX I: Some results on the Dubins minimum time solution

The goal of this section is to study arc-arc solutions that occur when the initial and final positions sufficiently separated. Specifically, we show that for each value of initial and final velocity vectors, there exists a minimum "separation" – denoted by l_c – between the initial and final positions beyond which there can only exist arc-line-arc solutions. Using the methods of this section it is possible to compute this

minimum separation (see Figure 8). This is useful in the numerical implementation of Dubins algorithm, as we can reject arc-arc-arc solutions apriori by simply checking the given separation against the critical one.

Choose coordinates so that the initial position is at the origin and the final position is on the positive x-axis. We hold ϕ_0 as fixed and vary the final angle ϕ_f and position $(l,0)$. For a given ϕ_0 value there exists two circles tangent to the initial velocity (denoted by A and B in Figure 7). A similar situation exists for the final position. In the following, we will consider angles ϕ_0 and ϕ_f modulo π radians. It can be seen in Figure 7 that rotation by π radians does not change the critical separation beyond which only arc-line-arc solutions exist. For a given ϕ_f value (with ϕ_0 already fixed), there exists a certain critical separation l_c that depends only on ϕ_0 and ϕ_f for which one of the circles tangent to the final velocity vector is tangent to one of the circles tangent to the initial velocity vector, *without any of the other circles intersecting each other.* For example, when $\phi_f \leq \phi_0$ the circles B and D can be made tangent (figure 7(a)) by systematically reducing l from a large value. Similarly, when $\phi_f > \phi_0 > \frac{\pi}{6}$ the circles B and C can be made tangent (figure 7(b)), by reducing l from a large value. It is clear that for values of l greater than the critical value l_c there only exist arc-line-arc solutions as one needs the tangent circles to intersect for an arc-arc-arc solution to exist (Dubins [8]).

The different possibilities when $\phi_0 \geq 0$ are shown in Figure 6 (see also Figure 7). Case 1 corresponds to combinations of ϕ_0 and ϕ_f such that circles B and D are tangential. Case 2 corresponds to combinations of ϕ_0 and ϕ_f such that circles B and C are tangential. Cases 3, 4 corresponds to combinations of ϕ_0, ϕ_f such that circles A and C are tangential. The difference between the two is in the computation of the critical separation. To be precise, angle $\alpha \leq \phi_f - \phi_0$ for Case 3, while $\phi_f - \phi_0 \leq \alpha$ for Case 4. For each of these cases, the computation of the critical separation has to be done using a different method. These are presented next.

Firstly, consider Case 1 that corresponds to $\phi_f \leq \phi_0$ (see figure 7(a)). In this case, the circles B and D are tangential. In ΔTSD, let $\angle STD = \beta$, $l(TD) = x$ and $l(TS) = l$. It is easy to see that $\angle TSD = \frac{\pi}{2} + \phi_f$. Applying the sine-rule to ΔTSD we get:

$$\frac{\cos(\phi_f)}{x} = \frac{\sin(\beta)}{r} = \frac{\cos(\phi_f + \beta)}{l}.$$

In ΔTSD, $\angle BTD = \frac{\pi}{2} - \phi_0 - \beta$. Applying the cosine rule:

$$4r^2 = r^2 + x^2 - 2rx\sin(\phi_0 + \beta).$$

We thus have two equations in two variables:

$$\begin{aligned} x\sin(\beta) - r\cos(\phi_f) &= 0 \\ x^2 - 2rx\sin(\phi_0 + \beta) - 3r^2 &= 0. \end{aligned}$$

We can employ an invertible coordinate change: $(x,\beta) \mapsto (y,z)$ given by $x\sin(\beta) = y$ and $x\cos(\beta) = z$. Then: $y = r\cos(\phi_f)$ and

$$z^2 - 2rz\sin(\phi_0) - 2ry\cos(\phi_0) + y^2 - 3r^2 = 0.$$

The latter equation is of the type: $z^2 + bz + c = 0$ with $b, c < 0$ which implies that there exist a unique positive and real solution z. This yields a unique solution for the critical separation l_c.

Secondly, consider Case 2 which is easiest to handle (figure 7(b)). In ΔOCS, $\angle CSO = \frac{\pi}{2} - \phi_f$. Let $\angle COS = \psi$ so that $\angle OCS = \frac{\pi}{2} + \phi_f - \psi$. Let $l(OC) = x_1$ and $l(OS) = l_1$. Applying the sine rule for triangles we get:

$$\frac{\sin(\psi)}{r} = \frac{\cos(\phi_f)}{x_1}.$$

Turning to ΔOBT, $\angle BTO = \frac{\pi}{2} - \phi_0$. Let $\angle BOT = \psi$ so that $\angle OBT = \frac{\pi}{2} + \phi_0 - \psi$. Let $l(OB) = x_2$ and $l(OS) = l_2$. As $x_1 + x_2 = 2r$, we get: $x_1 = \frac{2r\cos(\phi_f)}{\cos(\phi_0)+\cos(\phi_f)}$ and $x_2 = \frac{2r\cos(\phi_0)}{\cos(\phi_0)+\cos(\phi_f)}$. We can further solve for l_1 and l_2 and obtain $l = l_1 + l_2$ from:

$$l_1^2 = x_1^2 + r^2 + 2x_1 r\sin(\phi_f - \psi),$$
$$l_2^2 = x_2^2 + r^2 + 2x_2 r\sin(\phi_0 - \psi).$$

Thirdly, we consider Case 3, which consists of $0 \le \phi_0 \le \frac{\pi}{6}$ and $\phi_0 \le \phi_f \le \phi_f^{\#}$ (see Figure 7(c)). The angle $\phi_f^{\#}$ can be understood as follows. When $\phi_0 > 0$ and $\phi_f = 0$, the circles B and D become tangential first when l is reduced from a large value. As ϕ_f is increased from 0, it is found that when $\phi_f = \phi_0$, the circles $A - C$ and $B - D$ become tangential simultaneously with $l_c = 2r$, if and only if $0 \le \phi_0 \le \frac{\pi}{6}$. When $\phi_f = \phi_0 = \frac{\pi}{6}$, we have A,B and C tangent simultaneously and at the same time B, C and D are tangent simultaneously. If $\phi_0 > \frac{\pi}{6}$, it is not possible to make circles A and C tangent to each other without the other circles intersecting, for any angle ϕ_f[1] In the other case of $0 \le \phi_0 \le \frac{\pi}{6}$, there exists an angle ϕ_f^* for which circles A, B and C become tangential (see Figure 7(d)). Values of $\phi_f < \phi_f^*$ are further sub-divided into Cases 3 and 4 that depend on the relative position of the centers of the circles A, C and D. There exists an angle $\phi_f^{\#} \le \phi_f^*$ such that the centers of A, C and D collinear. We call the case $\phi_f \le \phi_f^{\#}$ as Case 3 and $\phi_f^{\#} \le \phi_f \le \phi_f^*$ as Case 4 (Figure 7(e)).
In ΔOAC:

$$\frac{\sin(\phi_f - \phi_0)}{2r} = \frac{\sin\alpha}{l(OC)} = \frac{\sin(\alpha - \phi_f + \phi_0)}{l(OA)}$$

In ΔATC:

$$\frac{\sin(\alpha+\gamma)}{2r} = \frac{\sin(\alpha)}{l(TC)} = \frac{\sin(\gamma)}{r}.$$

In ΔOTC:

$$\frac{\sin(\phi_f - \phi_0)}{l(TC)} = \frac{\sin(\alpha - \phi_f + \phi_0 + \gamma)}{r + l(OA)}.$$

[1] To be precise, if $l > 2r$ and $\phi_f = \phi_0 > \frac{\pi}{6}$, then B and C become tangential first leading to Case 2.

To find $l(TC)$ which is the critical separation, denote by $l_1 = l(OA)$): Also denote $z = [\alpha,\ \gamma,\ l_1]^T$. Then we have the equations:

$$f(z) = \begin{bmatrix} l_1 \sin(\phi_f - \phi_0) - 2r\sin(\alpha + \phi_0 - \phi_f) \\ \sin(\alpha+\gamma) - 2\sin(\gamma) \\ 2r\sin(\alpha+\gamma-\phi_f+\phi_0)\ \sin(\alpha) - (r+l_1)\ \sin(\alpha+\gamma)\ \sin(\phi_f - \phi_0) \end{bmatrix} = 0$$

We can solve for z using Newton's method and then compute $l(TC)$. A similar approach is used to compute $l(TC)$ in Case 4. The results of the computation can be found in Figure 8.

APPENDIX II: Basic Results on Optimal Control

The following is a specialization of Filippov's theorem [14] on the existence of minimum time optimal control for the system

$$\dot{q} = f(t,q,u) \tag{A-i}$$

where q and f are n dimensional vectors, u is r dimensional control parameter, which for every t and u takes values in a fixed *convex* set $U \subset \mathbb{R}^n$. The vector function $f(t,q,u)$ is continuous in all variables; differentiable a.e. with respect to q; and $q^T f(t,q,u) \leq C(\|q\|^2+1)$ for some $C > 0$, for all t and q, and all $u \in U$. Filippov's theorem [14] asks for continuous differentiability of $f(t,q,u)$ in the q variable, but a study of the proof shows that only differentiability a.e. is needed. By requiring $f(t,q,u)$ to be Lipschitz continuous in x is enough for Filippov's theorem to be true. By the continuity of f in the u variable, the set $R(t,q) = \{f(t,q,u)\,|\,u \in Q\}$ is a convex set for each t and q. For the system (A-i) satisfying the above conditions, consider the problem:

$$\min T \text{ such that } q(0) = q_0 \text{ and } q(T) = q^*. \tag{A-ii}$$

Theorem 2. *[14] Suppose that the conditions above are satisfied, and that there exists at least one measurable function $\tilde{u}$ with $\tilde{u}(t) \in U$ such that the solution $\bar{q}(t)$ with $u = \bar{u}(t)$ and initial condition $\bar{q}(0) = q_0$ attains q^* for some $t^* > 0$. Then there also exists an optimal control for Problem (A-ii), i.e., a measurable function $u(\cdot)$ with $u(t) \in U$.*

APPENDIX III: Maximum value of $\frac{(W_\parallel + \bar{V}_\parallel)^2}{|\bar{V}_\parallel|}$

Here, we will prove that:

$$\max_{V_\perp = -W_\perp} \frac{(W_\parallel + \bar{V}_\parallel)^2}{|\bar{V}_\parallel|} = \frac{(\|W\|_\infty + V)^2}{V}.$$

Denote: $x = \bar{V}_\parallel$ and $y = W_\parallel$. Then:

$$f(x) = \frac{(W_\parallel + \bar{V}_\parallel)^2}{|\bar{V}_\parallel|} = \frac{(y+x)^2}{x}.$$

As $W_\parallel = \sqrt{W^2 - V^2 + \bar{V}_\parallel^2}$ due to the condition $\bar{V}_\perp = -W_\perp$, we have:

$$f(x) = \frac{\|W\|_\infty^2 - V^2}{x} + 2\sqrt{\|W\|_\infty^2 - V^2 + x^2} + 2x.$$

The critical points where f takes its maximum or minimum values are points where $f'(x) = 0$ and the boundary points $x = V$, $x = \sqrt{V^2 - \|W\|_\infty^2}$.

Differentiating f with respect to x we get:

$$f'(x) = \frac{V^2 - \|W\|_\infty^2}{x^2} + \frac{2x}{\sqrt{\|W\|_\infty^2 - V^2 + x^2}} + 2.$$

For simplicity, denote $z = \frac{V^2 - \|W\|_\infty^2}{x^2}$. It is clear from Assumption A-1 that $z > 0$. Then:

$$F(z) = f'(x) = z + \frac{2}{\sqrt{1-z}} + 2.$$

Setting $F(z) = 0$ we get the two points: $z = 0$ or $z = -3$. As neither of these points lie in the domain of z, we check the value of $f(x)$ at the boundary points: $x_1 = V$ and $x_2 = \sqrt{V^2 - \|W\|_\infty^2}$. At x_1, $y = \sqrt{\|W\|_\infty^2 - V^2 + x^2} = \pm\|W\|_\infty$; while at x_2, $y = 0$. Comparing the values of $f(x_1)$ and $f(x_2)$, we find $f(x_1) > f(x_2)$. Therefore:

$$\max_{V_\perp = -W_\perp} \frac{(W_\parallel + \bar{V}_\parallel)^2}{|\bar{V}_\parallel|} = \frac{(\|W\|_\infty + V)^2}{V}.$$

5 Acknowledgement

R. Iyer was supported by ASEE/AFOSR Summer Faculty Fellowship and R. McNeely was supported by an AFRL Graduate Student Fellowship during the summer of 2005.

References

1. Chandler, P., Pachter, M., "Hierachical control for autonomous teams", AIAA-2001-4149, *Proc. AIAA Guidance, Navigation and Control Conference*, Montreal, Canada, August, 2001.
2. Schumacher, C., Chandler, P., Rasmussen, S., "Task allocation for wide area search munitions via network flow optimization", AIAA-2001-4147, *Proc. AIAA Guidance, Navigation and Control Conference*, Montreal, Canada, August, 2001.
3. Rasmussen, S., Mitchell, J. W., Chandler, P., Schumacher, C., Smith A. L., "Introduction to the MultiUAV2 simulation and its application to cooperative control research", FrB16.1, *Proc. Americal Control Conference*, Portland, OR, June, 2005.
4. Chaudhry, A. I., Misovec, K. M. , and DAndrea, R., "Low Observability Path Planning for an Unmanned Air Vehicle Using Mixed Integer Linear Programming"', *Proceedings of the 43rd IEEE Conference on Decision and Control*, Paradise Island, The Bahamas, December 2004.
5. Yang. G., Kapila, V., "Optimal path planning for unmanned air vehicles with kinematic and tactical constraints", WeA04-6, *Proc. 41st IEEE Conference on Decision and Control*, pp. 1301 – 1306, Las Vegas, NV, December 2002.
6. Howlett, J., "Path Planning for Sensing Multiple Targets from an Aircraft," *Masters Thesis*, Department of Mechanical Engineering, Brigham Young University, December 2002.
7. Anderson, E., "Extremal Control and Unmanned Air Vehicle Trajectory Generation," *Masters Thesis*, Department of Electrical and Computer Engineering, Brigham Young University, April 2002.
8. L. E. Dubins, "On curves of minimal length with a constraint on average curvature and with prescribed initial and terminal positions and tangents", *American Journal of Mathematics*, vol. 79, 1954, pp 497-516.
9. Savla, K., Bullo, F., Frazzoli, E., "On traveling salesperson problems for Dubins' vehicle: stochastic and dynamic environments", *Proc. IEEE Conf. on Decision and Control*, Seville, Spain, pages 4530-4535, December 2005.
10. McNeely, R., Iyer, R., Chandler, P., "Tour planning for an unmanned air vehicle", *Journal of Guidance, Control and Dynamics*, vol. 30, No. 5, pp. 1299-1306, 2007.
11. F. H. Clarke and Yu. S. Ledyaem and R. J. Stern and R. R. Wolenski, *Nonsmooth Analysis and Control Theory*, Springer Verlag, 1998.
12. Pontryagin, L. S., Boltyanskii, V. G., Gamkrelidze, R. V., and Mishchenko, E. F., *The Mathematical Theory of Optimal Processes*, John Wiley & Sons, Inc., New York, 1962, Authorized translation from the Russian by K. N. Trirogoff.
13. Betts, J. T., "Survey of Numerical Methods for Trajectory Optimization", *Journal of Guidance, Control and Dynamics*, Vol. 21, No. 2, March-April 1998, pp. 193–207.
14. Filippov, A. F., "On certain questions in the theory of optimal control", *SIAM Journal of Control*, Ser. A, Vol. 1, No. 1, 1962, pp. 76–84.

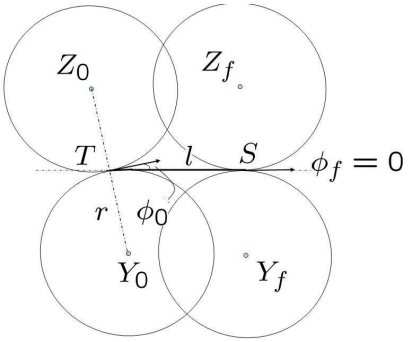

(a) A Y_0L solution for $\phi_f = 0$.

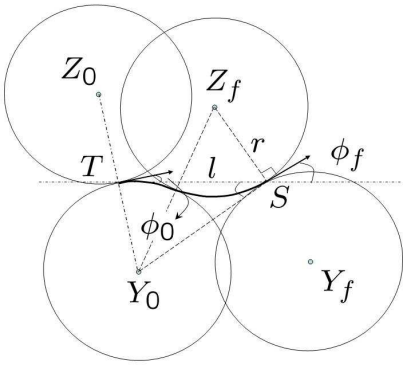

(b) A Y_0Z_f solution for $\phi_f = \bar{\phi}_c$.

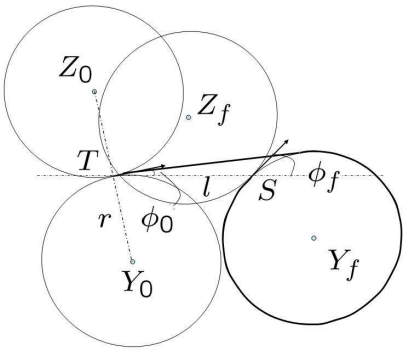

(c) A switch to a Z_0LY_f solution for $\phi_f > \bar{\phi}_c$.

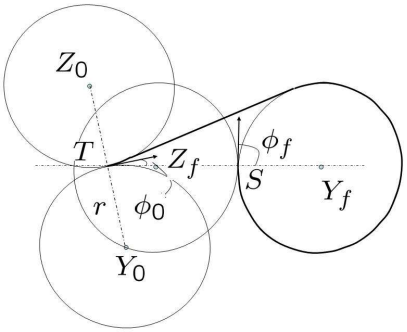

(d) A continuation of the previous case.

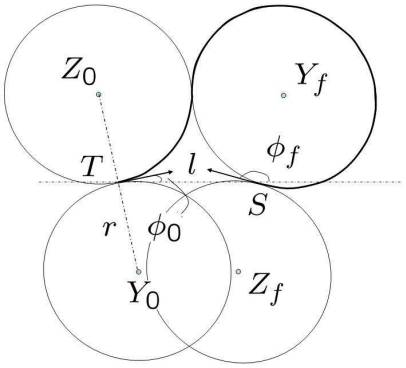

(e) A Z_0Y_f solution when $\phi_f = \tilde{\phi}_c$.

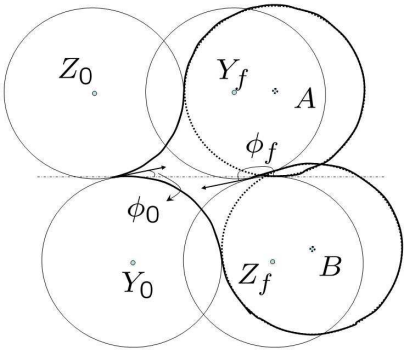

(f) Two arc-arc-arc Z_0AZ_f and Y_0BY_f solutions when $\phi_f = \phi_f^*$.

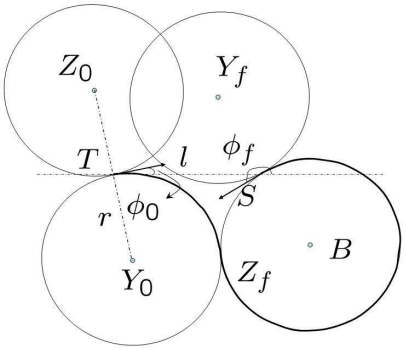

(g) A Y_0Z_f solution when $\phi_f = \hat{\phi}_c$.

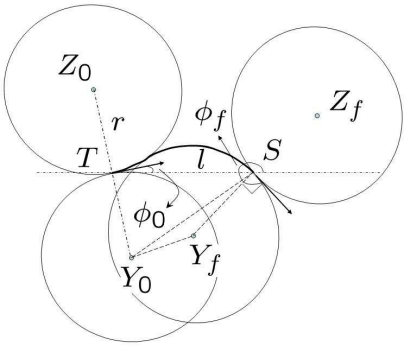

(h) A Z_0Y_f solution for $\phi_f = \bar{\phi}_c'$.

Fig. 2 Variation of the minimum time solution with ϕ_f for $0 < l < r(3 + |\sin\phi_0|)$.

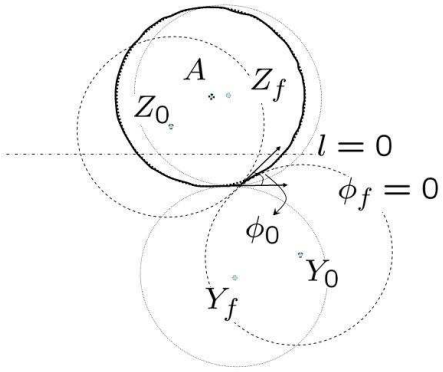

(a) An arc-arc-arc Y_0AY_f solution for $l = 0$, $|\phi_f - \phi_0| < \pi$.

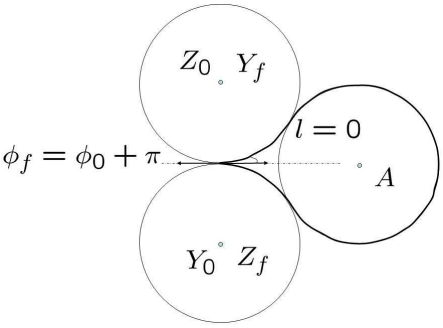

(b) Two arc-arc-arc Z_0AZ_f and Y_0AY_f solutions for $l = 0$, $\phi_f = \phi_0 + \pi$.

Fig. 3 Variation of the minimum time solution with the final angle ϕ_f for $l = 0$.

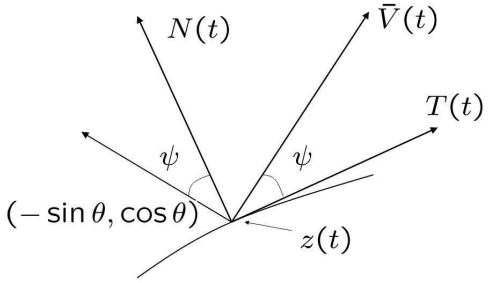

(a) Possibility 1.

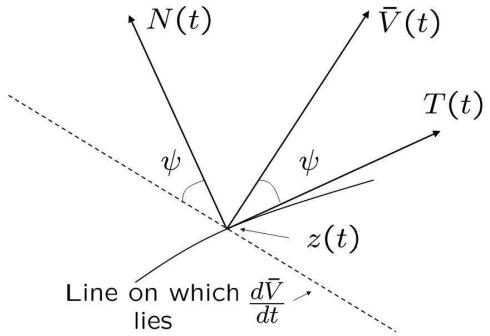

(b) Possibility 2.

Fig. 4 Relation between $\bar{V}$, N, and T.

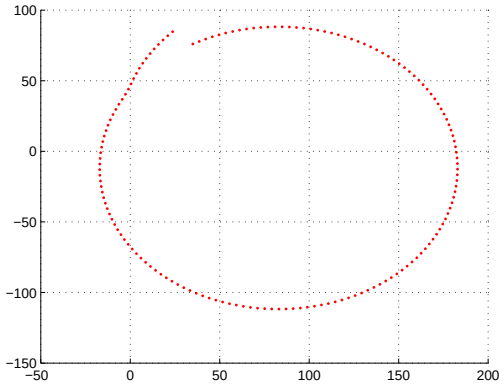

(a) Dubins Solution.

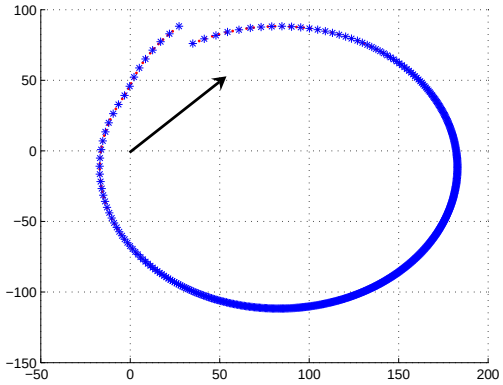

(b) Wind in 1st Quadrant.

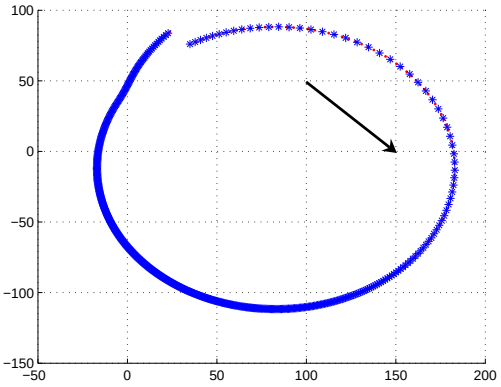

(c) Wind in 2nd Quadrant.

Fig. 5 Illustration of the construction of a solution for non-zero wind.

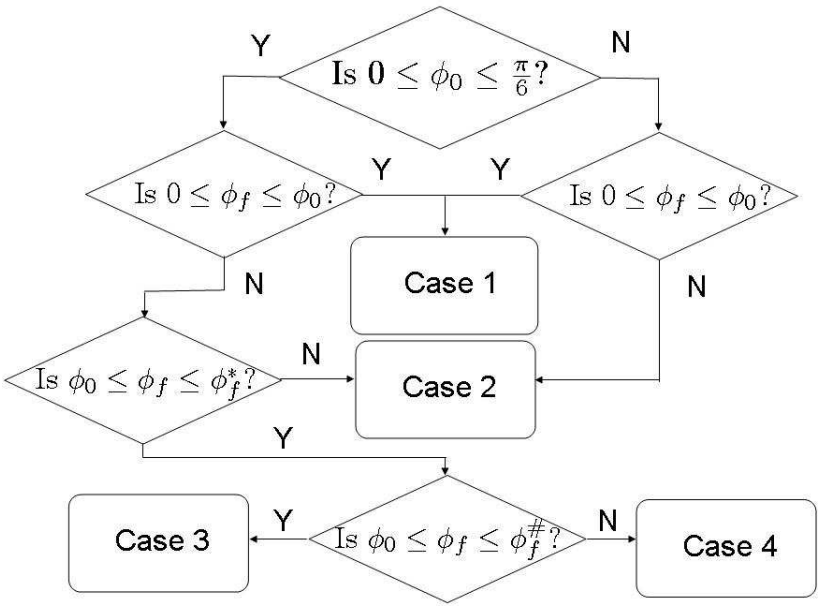

Fig. 6 Flow chart for the case $0 \leq \phi_0$.

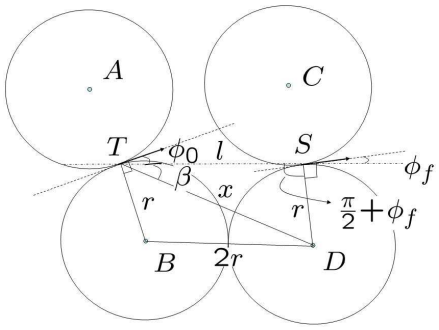

(a) Case 1: Circles B, D are tangential.

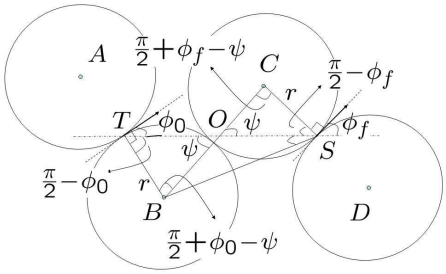

(b) Case 2: Circles B, C are tangential.

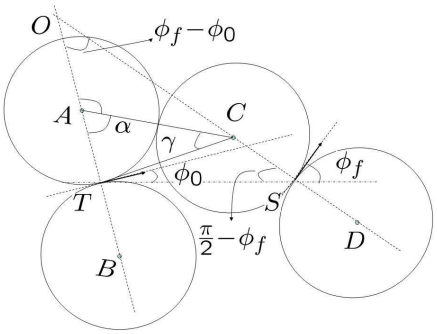

(c) Case 3: Circles A, C are tangential with $\phi_f - \phi_0 \leq \alpha$.

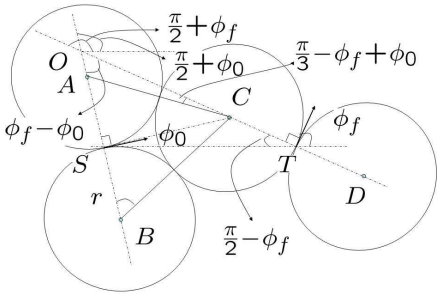

(d) Transition from Case 3 to Case 2 at $\phi_f = \phi_f^*$: Going from A and C tangential to B and C tangential.

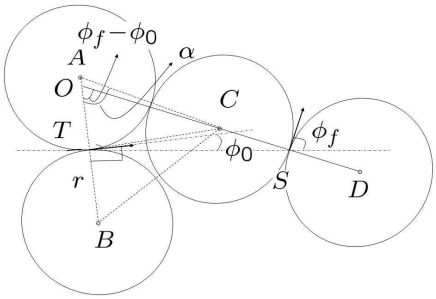

(e) Case 4: Circles A, C are tangential with $\alpha \leq \phi_f - \phi_0$.

Fig. 7 Study of arc-arc Dubins solutions.

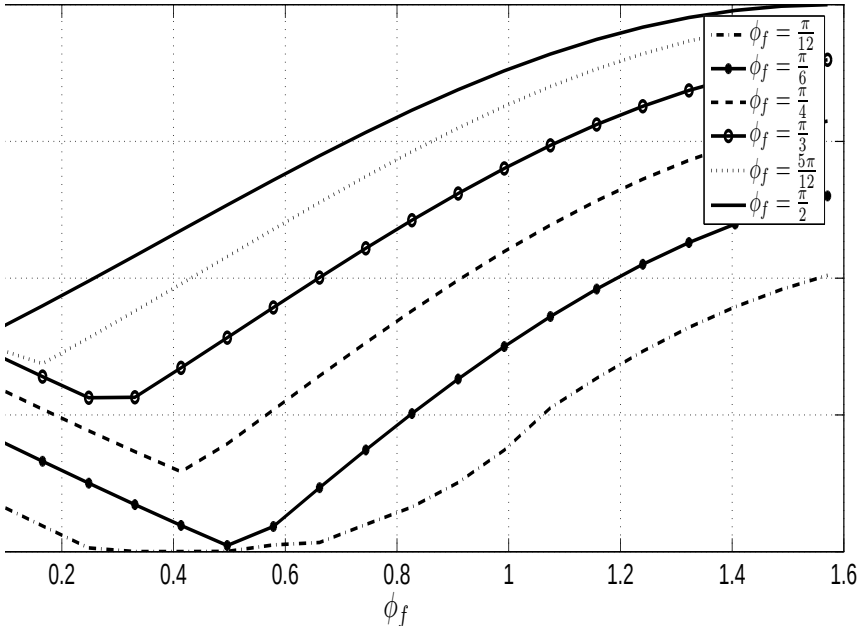

Fig. 8 Critical length to Radius ratios.